The effect of Gas Reaction Mixture on the Performance of CuO/Cu$_2$(OH)$_3$NO$_3$(Co^{2+}/Fe^{3+}) Composite Catalyst in the CO-PROX Reaction

Veselovskyi Volodymyr L.[*]**, Ischenko Elena V., Zakharova Tatyana M. and Lisnyak Vladyslav V.**[*]
Kyiv National Taras Shevchenko University, Kyiv 01601, UKRAINE

Abstract

The effect of gas reaction mixture composition on the performance of CuO/Cu$_2$(OH)$_3$NO$_3$(Co^{2+}/Fe^{3+}) composite catalyst in the CO-PROX reaction was examined. It was shown that the composition of the catalyst, which is formed at the pretreatment stage, changes with the increase of H$_2$ content in the reaction mixture. According to PXRD data the catalyst formed contains two phases: CuO and Cu$_2$(OH)$_3$NO$_3$, except that formed in the reaction mixture with excess of H$_2$ and deficiency of O$_2$, which contains three phases and possesses the lowest catalytic activity. Total CO conversion has been reached at 438 K and the selectivity towards CO oxidation was 94 % at this temperature. However, the composite catalyst has been found to be active and high selective only in the reaction mixture with a small excess of H$_2$. The selectivity towards CO oxidation has been sharply decreased with increase of H$_2$ content in the reaction mixture. The average particle size for composite catalyst studied was found to be about 20 nm. The increase of H$_2$ content in the reaction mixture did not much change the crystallite size of the composite catalyst components.

Keywords: CO-PROX, Cu$_2$(OH)$_3$NO$_3$, TPD MS, PXRD, SEM/EDX.

Introduction

It is known numerous routs that were applied in order to avoid contamination with different toxic substances[1-5]. The effect of pollutant traces on efficiency of proton exchange membrane fuel cells (PEMFC) has been reached much attention by scientists work in fields related to hydrogen energetics. The ideal fuel to feed PEMFC is hydrogen that could be produced by steam reforming, by partial oxidation or auto-thermal reforming of liquid fuels with further water-gas shift (WGS) reaction[6-9]. However, the hydrogen-rich reformate stream contains about 1 vol.% of CO traces that can adsorb on highly porous platinum anode, causing deterioration of the PEMFC[6-9]. The preferential oxidation of CO (CO-PROX) is proved to be one of the most effective methods to remove CO from the hydrogen-rich reformate stream[6-11].

An effective catalyst for CO-PROX reaction should be active in CO oxidation and selective enough towards CO oxidation in order to avoid undesired H$_2$ oxidation. This CO-PROX catalyst should operate in the same operation temperature range (353–473 K) as PEMFC and WGS[7-9]. Recent years researches devoted to preparation of effective CO-PROX catalysts have been directed mainly on combining different phases in the composite catalysts in order to reach high activity and selectivity in CO oxidation[6-11].

Earlier, CuO/Cu$_2$(OH)$_3$NO$_3$(Co^{2+}/Fe^{3+}) composite catalyst was examined in the low temperature CO conversion to CO$_2$[12,13]. The composite catalyst is formed at the pretreatment stage and contains a mix of two phases, namely: Cu$_2$(OH)$_3$NO$_3$ and CuO. It was shown that the addition of Co^{2+} and Fe^{3+} at the composite catalysts preparation stage stabilizes the Cu$_2$(OH)$_3$NO$_3$ phase in the composite and also improves overall catalytic activity in CO oxidation[9, 12, 13] and selectivity towards CO oxidation in a small excess of H$_2$[9]. The CuO/Cu$_2$(OH)$_3$NO$_3$(Co^{2+}/Fe^{3+}) composite catalyst was found to be promising candidate for the CO-PROX reaction due to its high activity and selectivity at relatively low temperatures. It could be mentioned that this composite is a desirable candidate due to low costs of starting materials used at the preparation if compare with more expensive noble metals catalysts[6, 10].

Activity and selectivity towards CO oxidation over the CuO/Cu$_2$(OH)$_3$NO$_3$(Co^{2+}/Fe^{3+}) composite catalyst in different gas reaction mixtures are reported in the present study. The composite catalyst prepared by a simple solution technique was characterized by N$_2$ physisorption, powder X-ray diffraction (PXRD), thermal program desorption followed by mass spectrometry (TPD MS) and by scanning electron microscopy with energy dispersive X-ray spectroscopy (SEM-EDX).

Material and Methods

Catalysts preparation: The Cu$_2$(OH)$_3$NO$_3$ doped with Co^{2+} and Fe^{3+} composite catalyst was prepared using the same preparation technique as reported[9, 12, 13] by dissolution of 1 g of mix of Cu, Co and Fe metals powders (all are Aldrich products) taken in the following mass ratio Cu : Co : Fe = 1 : 0.0526 : 0.0554. The sediment was recovered by filtration and transported to thermo-

programmed desiccator where was dried for 24 h at 373 K in an air atmosphere. In order to verify the reproducibility of the technique the catalyst was prepared at the same conditions numerous times.

Catalysts characterization: The specific surface area (S_{sp}) was determined by means of nitrogen physisorption at 77 K. The crystalline phases and average particle size of the catalyst were analyzed by powder X-ray diffraction (PXRD) measurements, which were carried out at room temperature using DRON-4-07 diffractometer (filtered $CoK\alpha_{1,2}$-radiation, λ = 1.7903 Å). Phases were identified by matching experimental patterns to the powder diffraction file[14], the crystal lattice parameters were evaluated using the UNITCELL program[15]. Estimation of phase quantity of PXRD data (EPQPXRD data) was performed using the reference intensity ratio method, which is based on I/I_c value, where I is the intensity of experimental PXRD pattern and I_c is the intensity of reference pattern. Average particle size was calculated from peak broadening using Scherrer equation:

$$\tau = \frac{K\lambda}{\beta cos\theta} \qquad (1)$$

where K is the shape factor (0.89), λ is the wavelength of radiation equals 1.7903 Å, β is the full width at half maxima (FWHM) in radians, and θ is the diffraction angle.

The chemical nature of the catalyst surface taken after the catalytic tests was examined by thermal program desorption followed by mass spectrometry measurements (TPD MS) using a quadrupole mass-spectrometer (MX-7304 A). The catalyst sample of 0.1 g was sealed in a quartz reactor connected with the mass-spectrometer. The sample was evacuated for *ca.* 1 · 10^{-4} Pa and then heated using a linear heating regime with 14 K/min rate in order to record the desorption runs of volatilized particles. These particles were then ionized and filtered selectively in the quadrupole by m/z. The m/z = 18 and 44 were monitored with the mass spectrometer as a function of the temperature. The CO_2 (m/z = 44) desorption energies (E_{des}) were calculated by the Amenomija-Cvetanovic method[16, 17]. A Jeol JSM-6490 scanning electron microscope equipped with an Oxford Inca 350 energy dispersive X-ray spectrometer (SEM-EDX) was used to study the morphology of catalysts and to perform elemental analysis.

Catalysts activity: The CO preferential oxidation was carried out in a continuous flow U-type microreactor at atmospheric pressure. An amount of 0.5 g of catalyst was placed on a calcined glass-fibers plate, fixed in the middle of the microreactor with 8 mm inside diameter. The reaction temperature was monitored by a Chromel/Alumel thermocouple placed in the catalyst bed formed by the sample tested. The composite catalyst was tested in gas reaction mixtures (GRMs) of different composition tabulated in table-1. Hereafter the notation used for the composite catalyst before the catalytic test is GRM(0) and the notation used for the catalyst tested is referred to the corresponding reaction mixture, *i.e.* GRM(1) is the first gas reaction mixture. The total gas flow rate of the reaction mixture was 100 mL/min. The concentration of CO and H_2 in the effluent gas was analyzed on-line by Shimadzu GC-2014 gas chromatograph with a molecular sieve 5A plot column equipped with a thermal conductivity detector (TCD).

The temperature at 100 % conversion of CO to CO_2 ($T_{100\%}$(CO)) was used as a measure of the catalytic activity. The catalytic test was performed in the temperature range from 300 K to whatever temperature was necessary to achieve complete CO conversion to CO_2 and then reduced to 300 K. The first temperature increase and further decrease is referred to the pretreatment stage. This procedure was then repeated for at least two times in order to reach a steady temperature at 100% CO conversion.

The CO and H_2 conversion calculation was based on the CO and H_2 consumption in the reaction as follows:

$$X_{CO}(\%) = \frac{C_{CO}^{in} - C_{CO}^{out}}{C_{CO}^{in}} \times 100 \qquad (2)$$

$$X_{H_2}(\%) = \frac{C_{H_2}^{in} - C_{H_2}^{out}}{C_{H_2}^{in}} \times 100 \qquad (3)$$

where in and out indexes correspond to inlet and outlet concentration of CO and H_2. The CO selectivity was calculated according to the following formula[1, 5]:

$$S(\%) = \frac{n\% \cdot X_{CO}}{n\% \cdot X_{CO} + m\% \cdot X_{H_2}} \times 100 \qquad (4)$$

where n and m are the volume percents of CO and H_2, respectively, in the GRM.

Results and Discussion

The specific surface area of the catalyst studied in different GRMs is found to be 8 $m^2 \cdot g^{-1}$.

Table-1
The composition of GRM and the phase content from QPXRD data

Reaction mixture	Composition of GRM				Phase content		
	CO, vol.%	O_2, vol.%	H_2, vol.%	He, vol.%	$Cu_2(OH)_3NO_3$, mass.%	CuO, mass.%	Cu, mass.%
GRM(0)	-	-	-	-	100	-	-
GRM(1)	2	2.5	1	94.5	60	40	-
GRM(2)	1	2.5	2	94.5	70	30	-
GRM(3)	1	2.5	20	76.5	40	20	40
GRM(4)	1	7.5	20	71.5	50	50	-

PXRD patterns of the composite catalyst are shown in figure-1. The composite catalyst before the catalytic test (*i.e.* GRM(0)) contains only the one phase indexed as the gerhardtite structure of $Cu_2(OH)_3NO_3$ (PDF No 00-045-0594, a = 5.66(3), b = 6.17(1), c = 7.07(1) Å, β = 92.36(1)°) for the sample taken before the catalytic test. No separate related oxide phases of Co^{2+} and Fe^{3+} dopants were found from the PXRD patterns due to their low concentration in the composite or due to the PXRD detection limit. Thus, the gerhardtite $Cu_2(OH)_3NO_3$ phase is the main phase in the composite catalyst before the catalytic test.

Prior to the catalytic test the composite catalyst was pretreated in the corresponding GRM. At the pretreatment stages the composite catalyst always showed a peak on the CO conversion versus temperature at 475–485 K displayed in figure-2. This peak could be explained by the decomposition of a part of $Cu_2(OH)_3NO_3$ to CuO at the noticed temperature range[4]. So, the composite catalyst formed at the pretreatment stage contains $Cu_2(OH)_3NO_3$ and CuO. It was shown earlier that the content of $Cu_2(OH)_3NO_3$ phase in the composite catalyst correlates with the catalytic activity in CO oxidation[7, 8]. The CO conversion and the selectivity towards CO oxidation over the composite catalyst tested in the different GRMs were represented on figure-3 and figure-4, correspondingly.

The composite catalyst tested in the GRM(1) shows $T_{100\%}(CO)$ at 433 K (S = 93 %). According to indexing of the PXRD pattern, the catalyst tested contains a mix of two crystalline phases: 60 mass.% of $Cu_2(OH)_3NO_3$ (a = 5.66(1), b = 6.16(1), c = 7.07(1) Å, γ = 92.94(1)°) and 40 mass.% of the tenorite structure CuO (PDF No. 00-005-0661, a = 4.69(1), b = 3.43(1), c = 5.14(1) Å, β = 99.56(1)°) and no reflections of other phases were registered.

The complete CO conversion over the composite catalyst tested in the GRM(2) is reached at 438 K (S = 94 %). This catalyst contains: 70 mass.% of $Cu_2(OH)_3NO_3$ (a = 5.67(1), b = 6.16(1), c = 7.09(1) Å, γ = 92.34(1)°) and 30 mass.% of CuO (a = 4.69(1), b = 3.43(1), c = 5.14(1) Å, β = 99.73(1)°). It should be mentioned that the CO oxidation over the catalyst in the GRM (1) and GRM(2) occurs at the temperature lower than that for the H_2 oxidation as tabulated in table-2.

According to data from the table-1, the content of crystalline phase of $Cu_2(OH)_3NO_3$ in the composite catalyst after the catalytic test increases with increase of H_2 content in the GRMs. However, the following increase of H_2 content in the reaction mixture up to 20 vol.% causes decrease of $Cu_2(OH)_3NO_3$ content in the composite catalyst. The composite catalyst tested in the GRM(3), according to indexing of the PXRD pattern, contains already a mix of three crystalline phases: 40 mass.% of $Cu_2(OH)_3NO_3$ (a = 5.63(1), b = 6.16(1), c = 7.05(1) Å, γ = 92.66(1)°), 20 mass.% of CuO (a = 4.68(1), b = 3.42(1), c = 5.11(1) Å, β = 99.58(1)°) and 40 mass.% of Cu ($a = b = c$ = 3.65(1) Å). It should be noted that the total CO conversion in this GRM has not been reached. This could be explained by lack

of O_2 and also by excess of H_2 in the GRM, which causes reduction of $Cu_2(OH)_3NO_3$ and/or CuO to metallic Cu.

The increase of O_2 content in the GRM enhances the catalytic activity of the composite. According to the PXRD data, the composite catalyst tested in the GRM(4) contains 50 mass.% of $Cu_2(OH)_3NO_3$ (a = 5.65(1), b = 6.16(1), c = 7.06(1) Å, γ = 92.46(1)°) and 50 mass.% of CuO (a = 4.69(1), b = 3.42(1), c = 5.13(1) Å, β = 99.68(1)°). According to figure-3, $T_{100\%}(CO)$ in the GRM(4) is 498 K (S = 8 %). The selectivity is very low if compare with that in the GRM(1) or GRM(2).

It was found that the Scherrer's crystallite size of CuO, $Cu_2(OH)_3NO_3$ and Cu phases is about 20 nm for the composite catalyst tested in the different GRMs. The pretreatment in the different GRMs, according to PXRD data, has no significant effect on the crystallite size of the composite catalyst components.

The typical form of the TPD MS profiles of H_2O and CO_2 is represented on figure-5. The most intensive TPD peaks of H_2O observed at 475–485 K is attributed to thermal degradation of $Cu_2(OH)_3NO_3$. The water most likely desorbs by direct recombination of -OH surface groups into H_2O. TPD-MS profiles of CO_2 show several peaks of CO_2 which correspond to several forms of CO_2. The latter desorbs in the molecular form from the catalyst surface. The calculated values of E_{des} and k at corresponding temperatures of CO_2 desorption are tabulated in the table-2. The values of E_{des} correlate very well with the catalyst activity in CO oxidation, namely: the lowest E_{des} corresponds to the most active catalyst.

The SEM micrographs recorded by photographing a single slow scan of the composite catalyst taken before and after the catalytic test in the GRM(2) are shown on figure-6 and figure-7, respectively. As one can see from the figure-6 and the figure-7, slice-like particles found in the initial catalysts sample are decomposed after the catalytic test and resulted particles are becoming more dispersed. The particles morphology seen on the SEM micrograph is typical for all samples tested in the different GRMs. According to the SEM-EDX microanalysis data displayed in figure-8, figure-9 and tabulated in table-3, the Cu : Co : Fe distribution in the composite catalyst grains is not homogenous.

The table-3 shows that the metals ratio in the catalyst studied before the catalytic test is found to be very different from that theoretical. So, one can suggest that Fe and Co are located mainly in the bulk of the catalyst. However, the metals ratio in the catalysts studied after the catalytic test is more close to the theoretical one. The increase of Fe and Co content found by SEM-EDX could be explained by the decomposition of a part of $Cu_2(OH)_3NO_3$ particles on the surface layer of the composite catalyst.
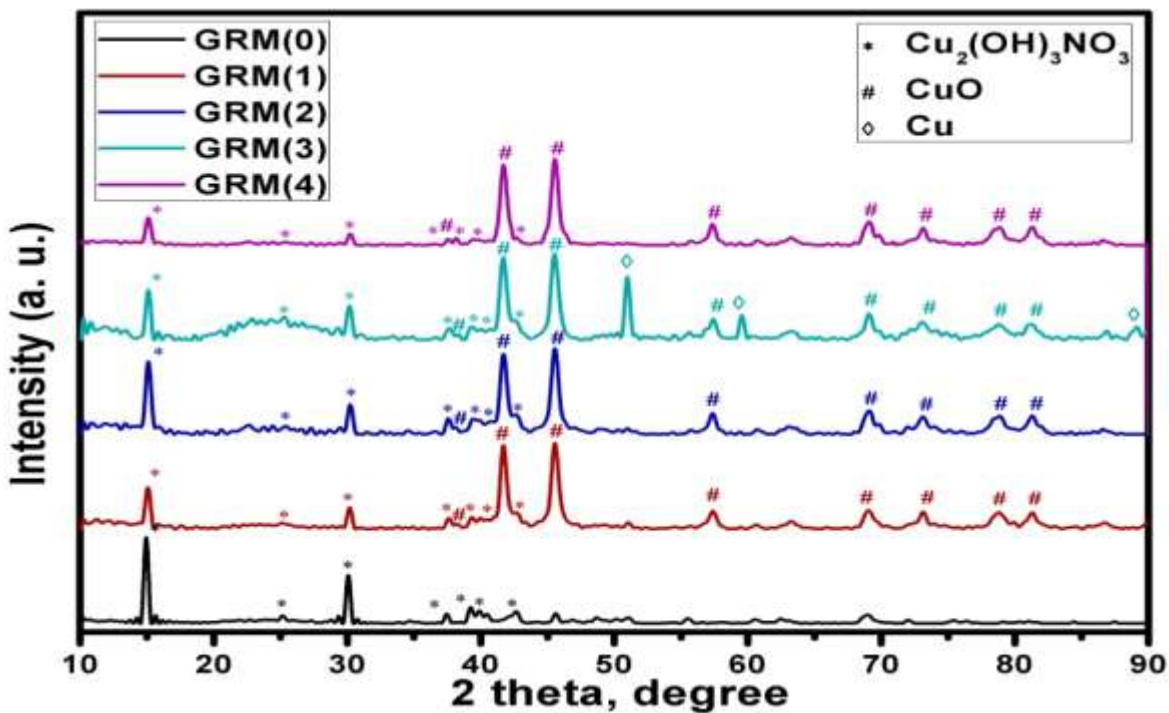
Figure-1
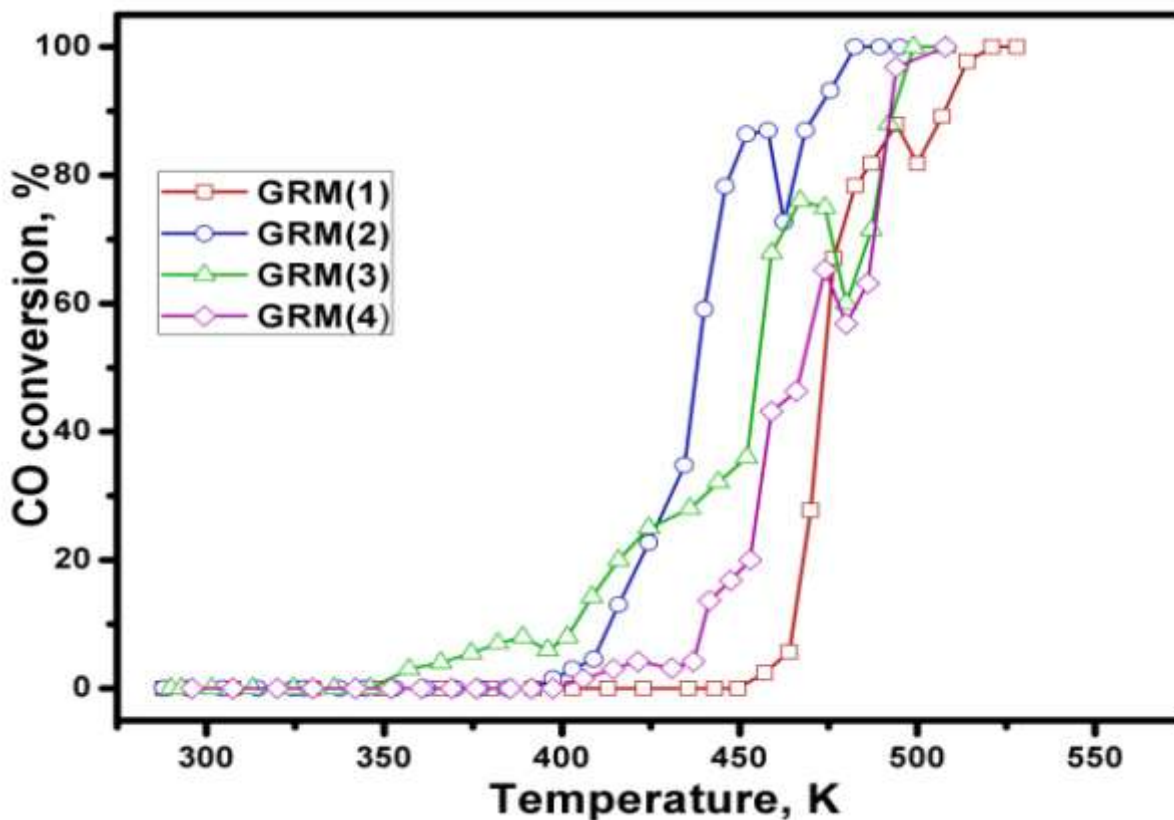**PXRD patterns of the composite catalyst studied before and after the catalytic tests**

Figure-2
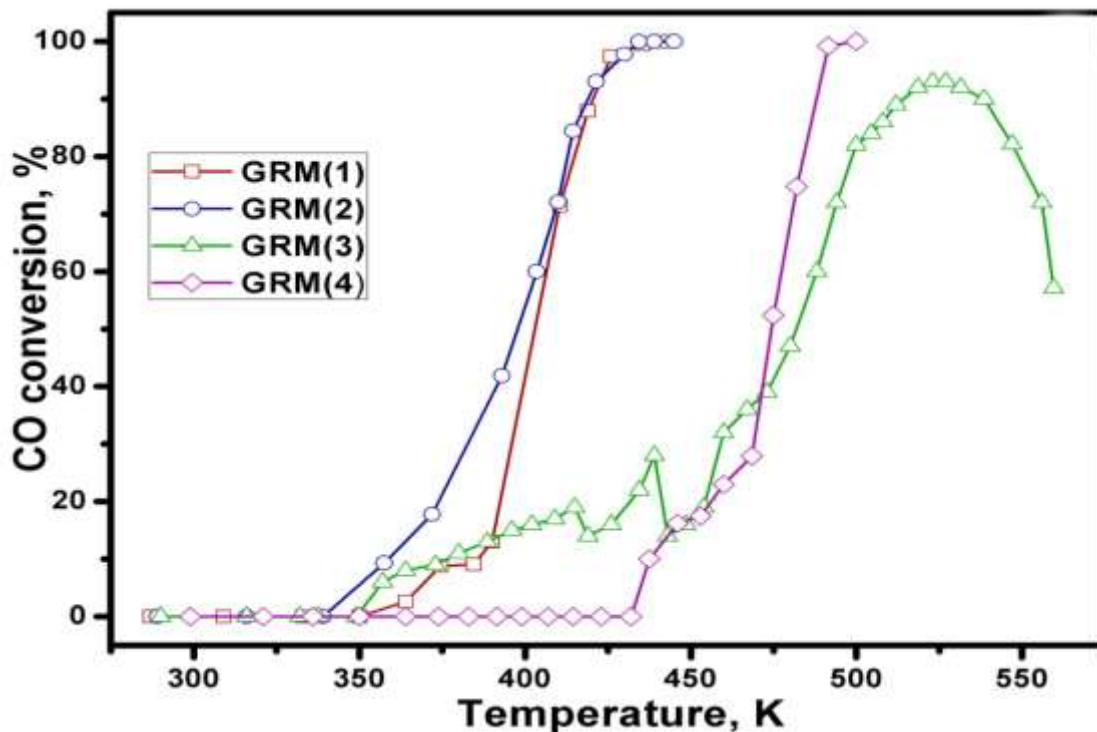**CO conversion over the composite catalyst pretreated in the different GRMs**

Figure-3
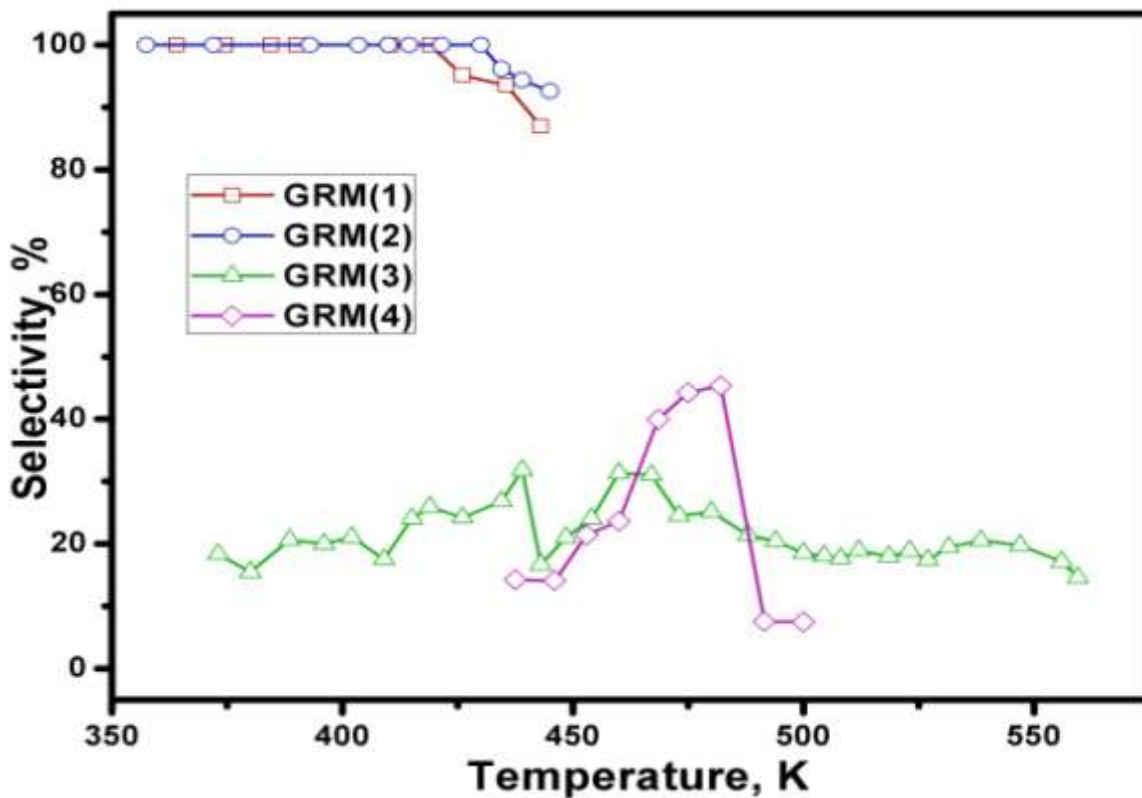**CO conversion over the composite catalyst tested in the different GRMs**

Figure-4
Selectivity over the composite catalyst tested in the different GRMs

Table-2
The temperature at 100 % conversion of CO to CO_2 ($T_{100\%}(CO)$), the selectivity (S) at $T_{100\%}(CO)$, the temperature of CO_2 desorption ($T_{des}(CO_2)$), pre-exponential factor (k) and the CO_2 desorption energy (E_{des})

Reaction mixture	$T_{100\%}(CO)$, K	S, %	TPD MS data		
			$T_{des}(CO_2)$, K	k	E_{des}, kJ · mol^{-1}
GRM(1)	433	93	453	$3.8 \cdot 10^8$	90.9
GRM(2)	438	94	468	$2.5 \cdot 10^9$	101.5
GRM(3)	518*	18*	458	$2.4 \cdot 10^{17}$	166.8
GRM(4)	498	8	478	$3.0 \cdot 10^{10}$	113.4

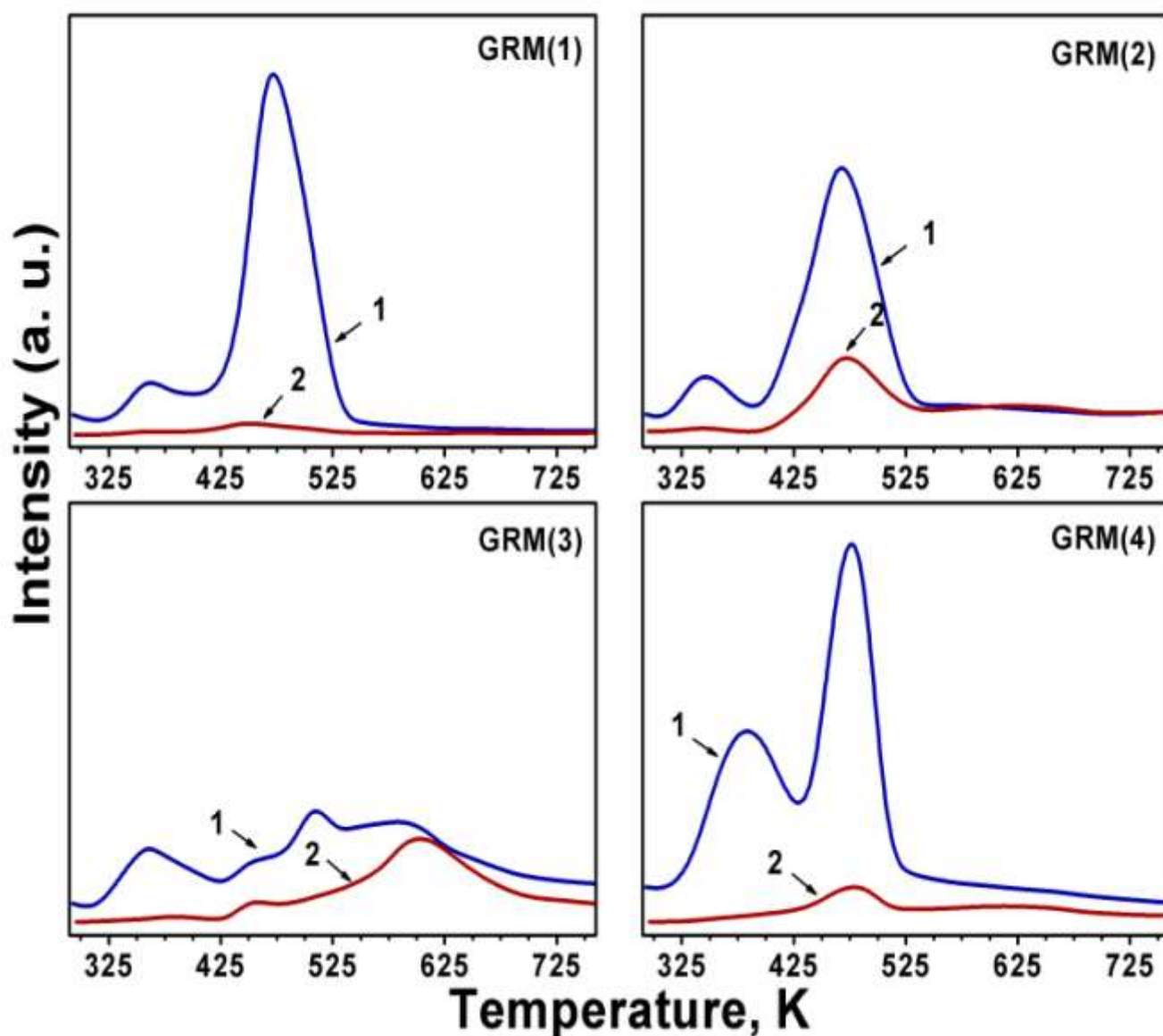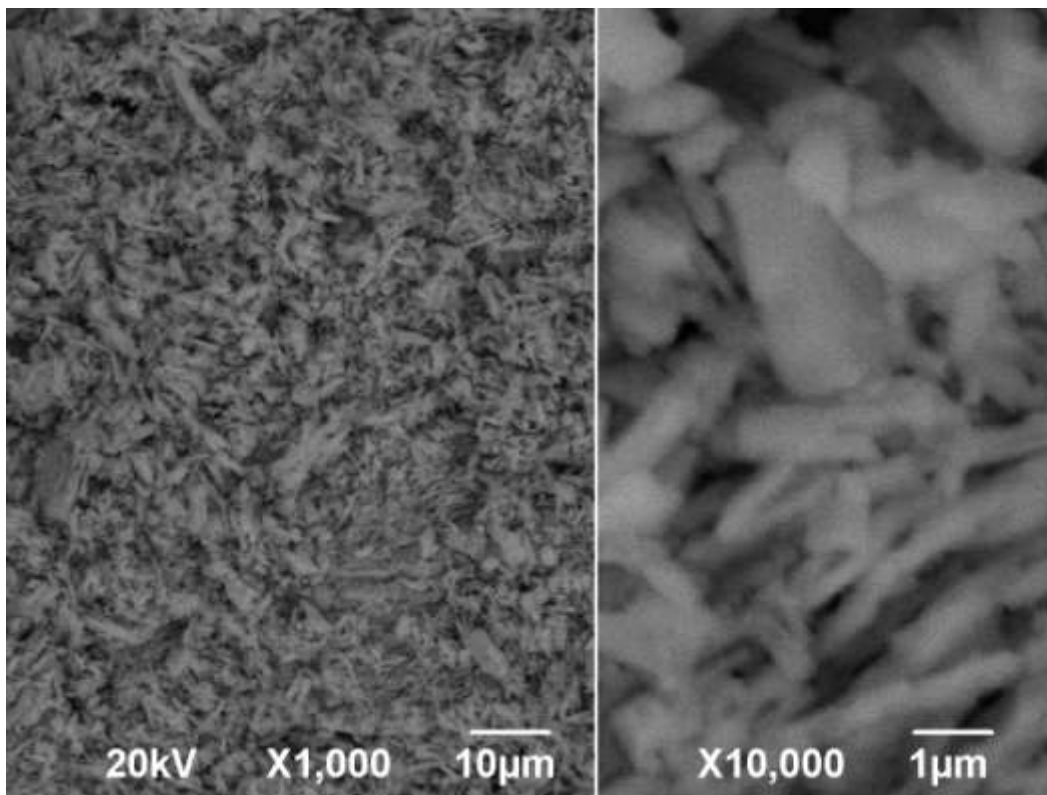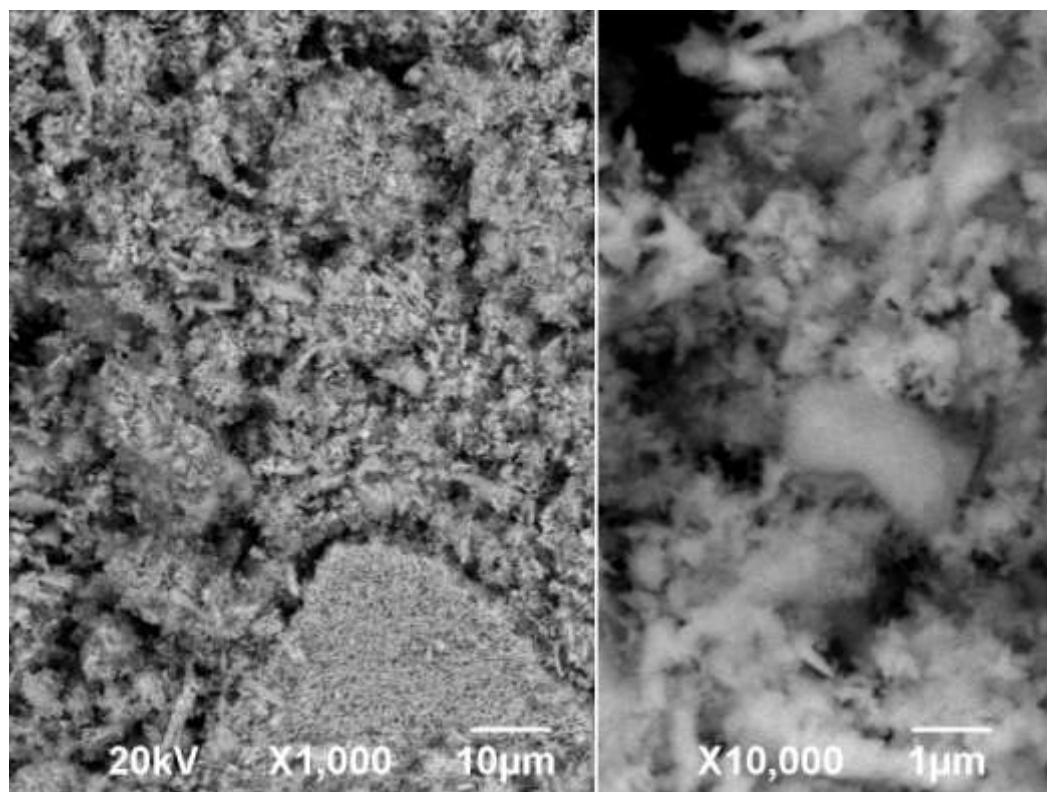* Note: the data are referred to the temperature of 96% CO conversion.

Figure-5
TPD MS profiles of *m/z* 18 (1) and 44 (2) for the catalyst tested in the different GRMs

Figure-6
The SEM micrographs of the catalyst studied before the catalytic test

Figure-7
The SEM micrographs of the catalyst studied after the catalytic test in the GRM(2)

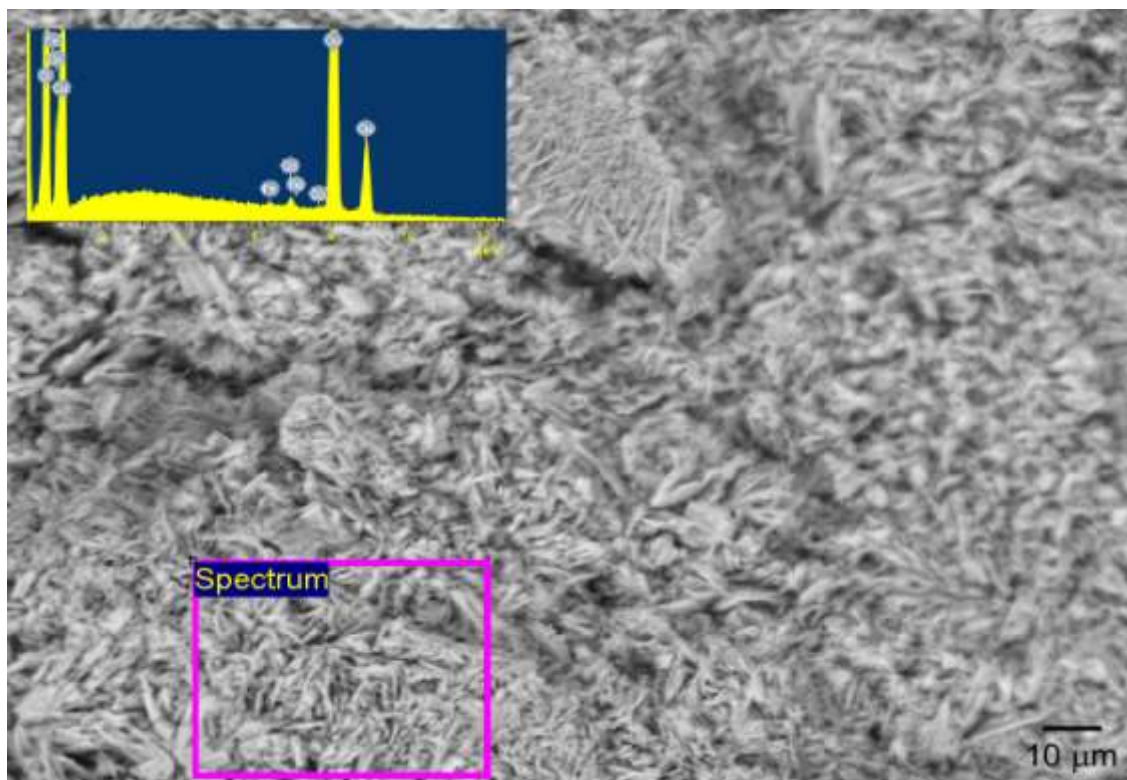**Figure-8**
The SEM-EDX elemental analysis of the catalyst studied before and after the catalytic test in the GRM(2).
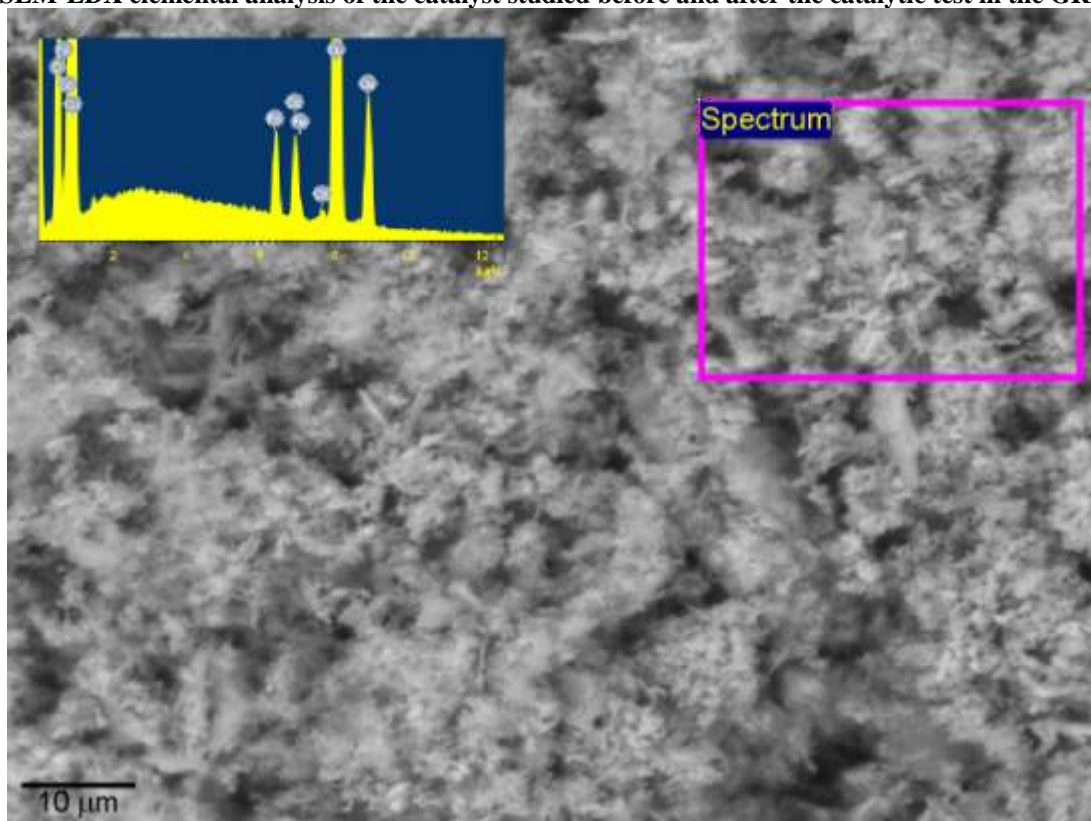

Figure-9
The SEM-EDX elemental analysis of the catalyst studied before and after the catalytic test in the GRM(2).

Table-3
The metals ratio in the composite catalyst

Reaction mixture	The metals ratio Cu : Co : Fe
Theoretical	1 : 0.0526 : 0.0554
GRM(0)	1 : 0.0082 : 0.0027
GRM(1)	1 : 0.0452 : 0.0381
GRM(2)	1 : 0.0410 : 0.0331
GRM(3)	1 : 0.0500 : 0.0457
GRM(4)	1 : 0.0481 : 0.0424

Conclusion

Summarizing, the catalyst is formed at the pretreatment stage, when $Cu_2(OH)_3NO_3$ phase partly decomposes to CuO and its morphology changes to more dispersed. According to PXRD data the catalyst formed contains two phases, except that formed in the GRM(3), which contains three phases and possesses the lowest catalytic activity. However, the composite catalyst has been found to be active and high selective only in the GRM with the oxygen deficiency. The selectivity towards CO oxidation has been sharply decreased with increase of H_2 content in the GRM. The activity decrease has been caused by the deficiency in O_2 in GRM(3) and GRM(4). Thus, this type of catalyst could be used in the CO-PROX reaction if GRM contains enough oxygen to avoid significant reduction of the active phases. $E_{des}(CO_2)$ values calculated from TPD MS profiles correlate well with the catalyst activity in different GRMs. No effect of increase of H_2 content on the crystallite size of the composite catalyst components was observed.

References

1. Sonawane V.Y., Mechanistic study of chromium (VI) catalyzed oxidation of benzyl alcohol by polymer supported chromic acid, *Res. J. Chem. Sci.*, **1**(**1**), 111-117 (**2011**)

2. Pandey Bh. and Fulekar M.H., Environmental Management - strategies for chemical disaster, *Res. J. Chem. Sci.*, **1**(**1**), 111-117 (**2011**)

3. Shivaraju H.P., Preparation and Characterization of Supported Photocatalytic Composite and its Decomposition and Disinfection Effect on Bacteria in Municipal Sewage Water, *Res. J. Chem. Sci.*, **1**(**2**), 56-63 (**2011**)

4. Rahul, Mathur A.K. and Balomajumder Ch., Biodegradation of Waste Gas containing Mixture of BTEX by B. Sphaericus, *Res. J. Chem. Sci.*, **1**(**5**), 52-60 (**2011**)

5. Thakur P.K., Rahul, Mathur A.K. and Balomajumder Ch., Biofiltration of Volatile Organic Compounds (VOCs) – An Overview, *Res. J. Chem. Sci.*, **1**(**8**), 83-92 (**2011**)

6. Sirichaiprasert K., Luengnaruemitchai A. and Pongstabodee S., Selective oxidation of CO to CO_2 over Cu–Ce–Fe–O composite-oxide catalyst in hydrogen feed stream, *Int. J. Hydrogen Energy*, **32**, 915-926 (**2007**)

7. Ayastuy J.L., Gurbani A., Gonzalez-Marcos M.P. and Gutierrez-Ortiz M.A., Effect of copper loading on copper-ceria catalysts performance in CO selective oxidation for fuel cell applications, *Int. J. Hydrogen Energy*, **35**, 1232-1244 (**2010**)

8. Zhao Zh., Lin X., Jin R., Dai Y, Wang G., High catalytic activity in CO PROX reaction of low cobalt-oxide loading catalysts supported on nano-particulate CeO_2–ZrO_2 oxides, *Catal. Commun.*, **12**, 1448-1451 (**2011**)

9. Veselovskyi V.L., Ischenko E.V., Gayday S.V. and Lisnyak V.V., A high efficient two phase $CuO/Cu_2(OH)_3NO_3(Co^{2+}/Fe^{3+})$ composite catalyst for CO-PROX reaction, *Catal. Commun.*, **18**, 137-141 (**2012**)

10. Qiao B., Zhang J., Liu L. and Deng Y., Low-temperature prepared highly effective ferric hydroxide supported gold catalysts for carbon monoxide selective oxidation in the presence of hydrogen, *Appl. Cat. A: Gen.*, **340**, 220-228 (**2008**)

11. Lendzion-Bielun Z., Bettahar M.M. and Monteverdi S., Fe-promoted CuO/CeO_2 catalyst Structural characterization and CO oxidation activity, *Catal. Commun.*, **11**, 1137-1142 (**2010**)

12. Yatsimirskii V.K., Maksimov Yu.V., Suzdalev I.P., Ishchenko E.V., Zakharenko N.I. and Gaidai S.V., Physical and chemical properties and activity of Fe-Co-Cu oxide catalysts in oxidation of CO, *Theor. Exper. Chem.*, **39**, 190-194 (**2003**)

13. Ischenko E.V., Yatsimirsky V.K., Dyachenko A.G., Borysenko M.V., Prilutskiy E.V. and Kongurova I.V., Cu-Co-Fe oxide catalysts supported on carbon nanotubes in the reaction of CO oxidation, *Polish J. Chem.*, **82**, 291-297 (**2008**)

14. PDF-2 Data Base JCPDS-ICDD 2007. JCPDS—International Centre for Diffraction Data: Newtown Square, PA, USA (**2007**)

15. Holland T.J.B. and Redfern S.A.T., Unit cell refinement from powder diffraction data; the use of regression diagnostics, *Mineral. Mag.*, **61**, 65-77(**1997**)

16. Cvetanovic R.J. and Amenomiya Y.A., Temperature programmed desorption technique for investigation of practical Catalysts, *Catal. Rev.*, **6**, 21-49 (**1972**)

17. Beda A.A. and Ishchenko E.V., Method for calculating kinetic parameters of the desorption for the case of incompletely resolved peaks in studying carbon nanotubes and silicon carbide, *J. Superhard Mater.*, **32**(**5**), 346-350 (**2010**)